arXiv:hep-ex/0408083v1 17 Aug 2004

Search for an $X(3872)$ Charged Partner in the Decay Mode $X^- \rightarrow J/\psi\pi^-\pi^0$ in the B Meson Decays $B^0 \rightarrow X^-K^+$ and $B^- \rightarrow X^-K^0_S$

The *BABAR* Collaboration

February 7, 2008

Abstract

We report on the search for a charged partner of the $X(3872)$ in the decay $B \rightarrow X^{\pm}K$, $X^{\pm} \rightarrow J/\psi\pi^{\pm}\pi^0$, using 213 million $B\overline{B}$ events collected at the $\Upsilon(4S)$ resonance with the *BABAR* detector at the PEP-II e^+e^- asymmetric-energy storage ring. The resulting product branching fraction upper limits are $\mathcal{B}(\bar{B}^0/B^0 \rightarrow X^{\pm}K^{\mp}, X^{\pm} \rightarrow J/\psi\pi^{\pm}\pi^0) < 5.8 \times 10^{-6}$ and $\mathcal{B}(B^{\pm} \rightarrow X^{\pm}K^0_S, X^{\pm} \rightarrow J/\psi\pi^{\pm}\pi^0) < 11 \times 10^{-6}$ at the 90% confidence level. All results are preliminary.

Submitted to the 32nd International Conference on High-Energy Physics, ICHEP 04,
16 August—22 August 2004, Beijing, China

The *BABAR* Collaboration,

B. Aubert, R. Barate, D. Boutigny, F. Couderc, J.-M. Gaillard, A. Hicheur, Y. Karyotakis, J. P. Lees,
V. Tisserand, A. Zghiche

Laboratoire de Physique des Particules, F-74941 Annecy-le-Vieux, France

A. Palano, A. Pompili

Università di Bari, Dipartimento di Fisica and INFN, I-70126 Bari, Italy

J. C. Chen, N. D. Qi, G. Rong, P. Wang, Y. S. Zhu

Institute of High Energy Physics, Beijing 100039, China

G. Eigen, I. Ofte, B. Stugu

University of Bergen, Inst. of Physics, N-5007 Bergen, Norway

G. S. Abrams, A. W. Borgland, A. B. Breon, D. N. Brown, J. Button-Shafer, R. N. Cahn, E. Charles,
C. T. Day, M. S. Gill, A. V. Gritsan, Y. Groysman, R. G. Jacobsen, R. W. Kadel, J. Kadyk, L. T. Kerth,
Yu. G. Kolomensky, G. Kukartsev, G. Lynch, L. M. Mir, P. J. Oddone, T. J. Orimoto, M. Pripstein,
N. A. Roe, M. T. Ronan, V. G. Shelkov, W. A. Wenzel

Lawrence Berkeley National Laboratory and University of California, Berkeley, CA 94720, USA

M. Barrett, K. E. Ford, T. J. Harrison, A. J. Hart, C. M. Hawkes, S. E. Morgan, A. T. Watson

University of Birmingham, Birmingham, B15 2TT, United Kingdom

M. Fritsch, K. Goetzen, T. Held, H. Koch, B. Lewandowski, M. Pelizaeus, M. Steinke

Ruhr Universität Bochum, Institut für Experimentalphysik 1, D-44780 Bochum, Germany

J. T. Boyd, N. Chevalier, W. N. Cottingham, M. P. Kelly, T. E. Latham, F. F. Wilson

University of Bristol, Bristol BS8 1TL, United Kingdom

T. Cuhadar-Donszelmann, C. Hearty, N. S. Knecht, T. S. Mattison, J. A. McKenna, D. Thiessen

University of British Columbia, Vancouver, BC, Canada V6T 1Z1

A. Khan, P. Kyberd, L. Teodorescu

Brunel University, Uxbridge, Middlesex UB8 3PH, United Kingdom

A. E. Blinov, V. E. Blinov, V. P. Druzhinin, V. B. Golubev, V. N. Ivanchenko, E. A. Kravchenko,
A. P. Onuchin, S. I. Serednyakov, Yu. I. Skovpen, E. P. Solodov, A. N. Yushkov

Budker Institute of Nuclear Physics, Novosibirsk 630090, Russia

D. Best, M. Bruinsma, M. Chao, I. Eschrich, D. Kirkby, A. J. Lankford, M. Mandelkern, R. K. Mommsen,
W. Roethel, D. P. Stoker

University of California at Irvine, Irvine, CA 92697, USA

C. Buchanan, B. L. Hartfiel

University of California at Los Angeles, Los Angeles, CA 90024, USA

S. D. Foulkes, J. W. Gary, B. C. Shen, K. Wang

University of California at Riverside, Riverside, CA 92521, USA

D. del Re, H. K. Hadavand, E. J. Hill, D. B. MacFarlane, H. P. Paar, Sh. Rahatlou, V. Sharma

University of California at San Diego, La Jolla, CA 92093, USA

J. W. Berryhill, C. Campagnari, B. Dahmes, O. Long, A. Lu, M. A. Mazur, J. D. Richman, W. Verkerke

University of California at Santa Barbara, Santa Barbara, CA 93106, USA

T. W. Beck, A. M. Eisner, C. A. Heusch, J. Kroseberg, W. S. Lockman, G. Nesom, T. Schalk,
B. A. Schumm, A. Seiden, P. Spradlin, D. C. Williams, M. G. Wilson

University of California at Santa Cruz, Institute for Particle Physics, Santa Cruz, CA 95064, USA

J. Albert, E. Chen, G. P. Dubois-Felsmann, A. Dvoretskii, D. G. Hitlin, I. Narsky, T. Piatenko,
F. C. Porter, A. Ryd, A. Samuel, S. Yang

California Institute of Technology, Pasadena, CA 91125, USA

S. Jayatilleke, G. Mancinelli, B. T. Meadows, M. D. Sokoloff

University of Cincinnati, Cincinnati, OH 45221, USA

T. Abe, F. Blanc, P. Bloom, S. Chen, W. T. Ford, U. Nauenberg, A. Olivas, P. Rankin, J. G. Smith,
J. Zhang, L. Zhang

University of Colorado, Boulder, CO 80309, USA

A. Chen, J. L. Harton, A. Soffer, W. H. Toki, R. J. Wilson, F. Winklmeier, Q. L. Zeng

Colorado State University, Fort Collins, CO 80523, USA

D. Altenburg, T. Brandt, J. Brose, M. Dickopp, E. Feltresi, A. Hauke, H. M. Lacker, R. Müller-Pfefferkorn,
R. Nogowski, S. Otto, A. Petzold, J. Schubert, K. R. Schubert, R. Schwierz, B. Spaan, J. E. Sundermann

Technische Universität Dresden, Institut für Kern- und Teilchenphysik, D-01062 Dresden, Germany

D. Bernard, G. R. Bonneaud, F. Brochard, P. Grenier, S. Schrenk, Ch. Thiebaux, G. Vasileiadis, M. Verderi

Ecole Polytechnique, LLR, F-91128 Palaiseau, France

D. J. Bard, P. J. Clark, D. Lavin, F. Muheim, S. Playfer, Y. Xie

University of Edinburgh, Edinburgh EH9 3JZ, United Kingdom

M. Andreotti, V. Azzolini, D. Bettoni, C. Bozzi, R. Calabrese, G. Cibinetto, E. Luppi, M. Negrini,
L. Piemontese, A. Sarti

Università di Ferrara, Dipartimento di Fisica and INFN, I-44100 Ferrara, Italy

E. Treadwell

Florida A&M University, Tallahassee, FL 32307, USA

F. Anulli, R. Baldini-Ferroli, A. Calcaterra, R. de Sangro, G. Finocchiaro, P. Patteri, I. M. Peruzzi,
M. Piccolo, A. Zallo

Laboratori Nazionali di Frascati dell'INFN, I-00044 Frascati, Italy

A. Buzzo, R. Capra, R. Contri, G. Crosetti, M. Lo Vetere, M. Macri, M. R. Monge, S. Passaggio,
C. Patrignani, E. Robutti, A. Santroni, S. Tosi

Università di Genova, Dipartimento di Fisica and INFN, I-16146 Genova, Italy

S. Bailey, G. Brandenburg, K. S. Chaisanguanthum, M. Morii, E. Won

Harvard University, Cambridge, MA 02138, USA

3

R. S. Dubitzky, U. Langenegger

Universität Heidelberg, Physikalisches Institut, Philosophenweg 12, D-69120 Heidelberg, Germany

W. Bhimji, D. A. Bowerman, P. D. Dauncey, U. Egede, J. R. Gaillard, G. W. Morton, J. A. Nash, M. B. Nikolich, G. P. Taylor

Imperial College London, London, SW7 2AZ, United Kingdom

M. J. Charles, G. J. Grenier, U. Mallik

University of Iowa, Iowa City, IA 52242, USA

J. Cochran, H. B. Crawley, J. Lamsa, W. T. Meyer, S. Prell, E. I. Rosenberg, A. E. Rubin, J. Yi

Iowa State University, Ames, IA 50011-3160, USA

M. Biasini, R. Covarelli, M. Pioppi

Università di Perugia, Dipartimento di Fisica and INFN, I-06100 Perugia, Italy

M. Davier, X. Giroux, G. Grosdidier, A. Höcker, S. Laplace, F. Le Diberder, V. Lepeltier, A. M. Lutz, T. C. Petersen, S. Plaszczynski, M. H. Schune, L. Tantot, G. Wormser

Laboratoire de l'Accélérateur Linéaire, F-91898 Orsay, France

C. H. Cheng, D. J. Lange, M. C. Simani, D. M. Wright

Lawrence Livermore National Laboratory, Livermore, CA 94550, USA

A. J. Bevan, C. A. Chavez, J. P. Coleman, I. J. Forster, J. R. Fry, E. Gabathuler, R. Gamet, D. E. Hutchcroft, R. J. Parry, D. J. Payne, R. J. Sloane, C. Touramanis

University of Liverpool, Liverpool L69 72E, United Kingdom

J. J. Back,[1] C. M. Cormack, P. F. Harrison,[1] F. Di Lodovico, G. B. Mohanty[1]

Queen Mary, University of London, E1 4NS, United Kingdom

C. L. Brown, G. Cowan, R. L. Flack, H. U. Flaecher, M. G. Green, P. S. Jackson, T. R. McMahon, S. Ricciardi, F. Salvatore, M. A. Winter

University of London, Royal Holloway and Bedford New College, Egham, Surrey TW20 0EX, United Kingdom

D. Brown, C. L. Davis

University of Louisville, Louisville, KY 40292, USA

J. Allison, N. R. Barlow, R. J. Barlow, P. A. Hart, M. C. Hodgkinson, G. D. Lafferty, A. J. Lyon, J. C. Williams

University of Manchester, Manchester M13 9PL, United Kingdom

A. Farbin, W. D. Hulsbergen, A. Jawahery, D. Kovalskyi, C. K. Lae, V. Lillard, D. A. Roberts

University of Maryland, College Park, MD 20742, USA

G. Blaylock, C. Dallapiccola, K. T. Flood, S. S. Hertzbach, R. Kofler, V. B. Koptchev, T. B. Moore, S. Saremi, H. Staengle, S. Willocq

University of Massachusetts, Amherst, MA 01003, USA

---

[1]Now at Department of Physics, University of Warwick, Coventry, United Kingdom

R. Cowan, G. Sciolla, S. J. Sekula, F. Taylor, R. K. Yamamoto

Massachusetts Institute of Technology, Laboratory for Nuclear Science, Cambridge, MA 02139, USA

D. J. J. Mangeol, P. M. Patel, S. H. Robertson

McGill University, Montréal, QC, Canada H3A 2T8

A. Lazzaro, V. Lombardo, F. Palombo

Università di Milano, Dipartimento di Fisica and INFN, I-20133 Milano, Italy

J. M. Bauer, L. Cremaldi, V. Eschenburg, R. Godang, R. Kroeger, J. Reidy, D. A. Sanders, D. J. Summers, H. W. Zhao

University of Mississippi, University, MS 38677, USA

S. Brunet, D. Côté, P. Taras

Université de Montréal, Laboratoire René J. A. Lévesque, Montréal, QC, Canada H3C 3J7

H. Nicholson

Mount Holyoke College, South Hadley, MA 01075, USA

N. Cavallo, F. Fabozzi,[2] C. Gatto, L. Lista, D. Monorchio, P. Paolucci, D. Piccolo, C. Sciacca

Università di Napoli Federico II, Dipartimento di Scienze Fisiche and INFN, I-80126, Napoli, Italy

M. Baak, H. Bulten, G. Raven, H. L. Snoek, L. Wilden

NIKHEF, National Institute for Nuclear Physics and High Energy Physics, NL-1009 DB Amsterdam, The Netherlands

C. P. Jessop, J. M. LoSecco

University of Notre Dame, Notre Dame, IN 46556, USA

T. Allmendinger, K. K. Gan, K. Honscheid, D. Hufnagel, H. Kagan, R. Kass, T. Pulliam, A. M. Rahimi, R. Ter-Antonyan, Q. K. Wong

Ohio State University, Columbus, OH 43210, USA

J. Brau, R. Frey, O. Igonkina, C. T. Potter, N. B. Sinev, D. Strom, E. Torrence

University of Oregon, Eugene, OR 97403, USA

F. Colecchia, A. Dorigo, F. Galeazzi, M. Margoni, M. Morandin, M. Posocco, M. Rotondo, F. Simonetto, R. Stroili, G. Tiozzo, C. Voci

Università di Padova, Dipartimento di Fisica and INFN, I-35131 Padova, Italy

M. Benayoun, H. Briand, J. Chauveau, P. David, Ch. de la Vaissière, L. Del Buono, O. Hamon, M. J. J. John, Ph. Leruste, J. Malcles, J. Ocariz, M. Pivk, L. Roos, S. T'Jampens, G. Therin

Universités Paris VI et VII, Laboratoire de Physique Nucléaire et de Hautes Energies, F-75252 Paris, France

P. F. Manfredi, V. Re

Università di Pavia, Dipartimento di Elettronica and INFN, I-27100 Pavia, Italy

---

[2]Also with Università della Basilicata, Potenza, Italy

P. K. Behera, L. Gladney, Q. H. Guo, J. Panetta

University of Pennsylvania, Philadelphia, PA 19104, USA

C. Angelini, G. Batignani, S. Bettarini, M. Bondioli, F. Bucci, G. Calderini, M. Carpinelli, F. Forti, M. A. Giorgi, A. Lusiani, G. Marchiori, F. Martinez-Vidal,[3] M. Morganti, N. Neri, E. Paoloni, M. Rama, G. Rizzo, F. Sandrelli, J. Walsh

Università di Pisa, Dipartimento di Fisica, Scuola Normale Superiore and INFN, I-56127 Pisa, Italy

M. Haire, D. Judd, K. Paick, D. E. Wagoner

Prairie View A&M University, Prairie View, TX 77446, USA

N. Danielson, P. Elmer, Y. P. Lau, C. Lu, V. Miftakov, J. Olsen, A. J. S. Smith, A. V. Telnov

Princeton University, Princeton, NJ 08544, USA

F. Bellini, G. Cavoto,[4] R. Faccini, F. Ferrarotto, F. Ferroni, M. Gaspero, L. Li Gioi, M. A. Mazzoni, S. Morganti, M. Pierini, G. Piredda, F. Safai Tehrani, C. Voena

Università di Roma La Sapienza, Dipartimento di Fisica and INFN, I-00185 Roma, Italy

S. Christ, G. Wagner, R. Waldi

Universität Rostock, D-18051 Rostock, Germany

T. Adye, N. De Groot, B. Franek, N. I. Geddes, G. P. Gopal, E. O. Olaiya

Rutherford Appleton Laboratory, Chilton, Didcot, Oxon, OX11 0QX, United Kingdom

R. Aleksan, S. Emery, A. Gaidot, S. F. Ganzhur, P.-F. Giraud, G. Hamel de Monchenault, W. Kozanecki, M. Legendre, G. W. London, B. Mayer, G. Schott, G. Vasseur, Ch. Yèche, M. Zito

DSM/Dapnia, CEA/Saclay, F-91191 Gif-sur-Yvette, France

M. V. Purohit, A. W. Weidemann, J. R. Wilson, F. X. Yumiceva

University of South Carolina, Columbia, SC 29208, USA

D. Aston, R. Bartoldus, N. Berger, A. M. Boyarski, O. L. Buchmueller, R. Claus, M. R. Convery, M. Cristinziani, G. De Nardo, D. Dong, J. Dorfan, D. Dujmic, W. Dunwoodie, E. E. Elsen, S. Fan, R. C. Field, T. Glanzman, S. J. Gowdy, T. Hadig, V. Halyo, C. Hast, T. Hryn'ova, W. R. Innes, M. H. Kelsey, P. Kim, M. L. Kocian, D. W. G. S. Leith, J. Libby, S. Luitz, V. Luth, H. L. Lynch, H. Marsiske, R. Messner, D. R. Muller, C. P. O'Grady, V. E. Ozcan, A. Perazzo, M. Perl, S. Petrak, B. N. Ratcliff, A. Roodman, A. A. Salnikov, R. H. Schindler, J. Schwiening, G. Simi, A. Snyder, A. Soha, J. Stelzer, D. Su, M. K. Sullivan, J. Va'vra, S. R. Wagner, M. Weaver, A. J. R. Weinstein, W. J. Wisniewski, M. Wittgen, D. H. Wright, A. K. Yarritu, C. C. Young

Stanford Linear Accelerator Center, Stanford, CA 94309, USA

P. R. Burchat, A. J. Edwards, T. I. Meyer, B. A. Petersen, C. Roat

Stanford University, Stanford, CA 94305-4060, USA

S. Ahmed, M. S. Alam, J. A. Ernst, M. A. Saeed, M. Saleem, F. R. Wappler

State University of New York, Albany, NY 12222, USA

---

[3]Also with IFIC, Instituto de Física Corpuscular, CSIC-Universidad de Valencia, Valencia, Spain
[4]Also with Princeton University, Princeton, USA

W. Bugg, M. Krishnamurthy, S. M. Spanier

University of Tennessee, Knoxville, TN 37996, USA

R. Eckmann, H. Kim, J. L. Ritchie, A. Satpathy, R. F. Schwitters

University of Texas at Austin, Austin, TX 78712, USA

J. M. Izen, I. Kitayama, X. C. Lou, S. Ye

University of Texas at Dallas, Richardson, TX 75083, USA

F. Bianchi, M. Bona, F. Gallo, D. Gamba

Università di Torino, Dipartimento di Fisica Sperimentale and INFN, I-10125 Torino, Italy

L. Bosisio, C. Cartaro, F. Cossutti, G. Della Ricca, S. Dittongo, S. Grancagnolo, L. Lanceri, P. Poropat,[5]
L. Vitale, G. Vuagnin

Università di Trieste, Dipartimento di Fisica and INFN, I-34127 Trieste, Italy

R. S. Panvini

Vanderbilt University, Nashville, TN 37235, USA

Sw. Banerjee, C. M. Brown, D. Fortin, P. D. Jackson, R. Kowalewski, J. M. Roney, R. J. Sobie

University of Victoria, Victoria, BC, Canada V8W 3P6

H. R. Band, B. Cheng, S. Dasu, M. Datta, A. M. Eichenbaum, M. Graham, J. J. Hollar, J. R. Johnson,
P. E. Kutter, H. Li, R. Liu, A. Mihalyi, A. K. Mohapatra, Y. Pan, R. Prepost, P. Tan, J. H. von
Wimmersperg-Toeller, J. Wu, S. L. Wu, Z. Yu

University of Wisconsin, Madison, WI 53706, USA

M. G. Greene, H. Neal

Yale University, New Haven, CT 06511, USA

---

[5]Deceased

1 INTRODUCTION

Since the discovery of the $X(3872)$ by the Belle Collaboration [1], there have been experimental confirmations from the CDF [2], D0 [3] and *BABAR* [4] Collaborations. Numerous theoretical explanations have been proposed for this high-mass, narrow-width state decaying into $J/\psi\pi^+\pi^-$. The possibilities [5] include a charmonium state [6], a meson molecular state [7], and a hybrid charmonium state [8]. The Cornell potential model [9] predicts a charmonium state, previously unseen, with quantum numbers $n^{2S+1}L_J=1^3D_2$ and $J^{PC} = 2^{--}$. Also this charmonium state should be a narrow width state with a 3.830 GeV mass and have a large radiative transition rate, $X(3872) \to \gamma\chi_{c1}$, which has not been observed by Belle [1]. Since the measured $X(3872)$ mass is very close to the $D^{*0}\bar{D}^0$ mass threshold, another attractive possibility is a molecular model which is a bound state of mesons. If such states exist, then bound states of charged and neutral mesons or charged molecular states are plausible.

The $\pi^+\pi^-$ mass distributions from the $X(3872)$ decay measured by Belle [1] and *BABAR* [4], both peak near the kinematic upper limit and may be consistent with the decay of $\rho^0 \to \pi^+\pi^-$. However, due to limited statistics a spin-parity analysis has not been performed. If indeed, the observed decay is $X(3872) \to J/\psi\rho^0$, then a charged partner, $X(3872)^\pm \to J/\psi\rho^\pm$, may exist. Assuming the X charged partner is a member of an isotriplet and isospin is conserved in the B decays, the decay rate of $B \to X^\pm K$ should be twice that of $B \to X^0 K$. This would make experimental detection of the $X^\pm$ quite favorable. To test this conjecture, the *BABAR* collaboration has performed a search, presented in this paper, for the B-meson decays, $\bar{B}^0/B^0 \to X^\pm K^\mp$ and $B^\pm \to X^\pm K_S^0$, where $X^\pm \to J/\psi\pi^\pm\pi^0$.

2 THE *BABAR* DETECTOR AND DATASET

The data used in this analysis correspond to a total integrated luminosity of 193 fb^{-1} taken on the $\Upsilon(4S)$ resonance, producing a sample of 213.2$\pm$2.3 million $B\bar{B}$ events ($N_{B\bar{B}}$). Data were collected at the PEP-II asymmetric-energy e^+e^- storage ring with the *BABAR* detector, which is described in detail elsewhere [10]. The *BABAR* detector includes a silicon vertex tracker (SVT) and a drift chamber (DCH) in a 1.5 Tesla solenoidal magnetic field to detect charged particles and measure their momenta and energy loss (dE/dx). Photons, electrons, and neutral hadrons are detected in a CsI(Tl)-crystal electromagnetic calorimeter (EMC). An internally reflecting ring-imaging Cherenkov detector (DIRC) provides particle identification information that is complementary to that from dE/dx. Penetrating muons and neutral hadrons are identified by resistive-plate chambers in the steel flux return (IFR). Preliminary track-selection criteria in this analysis follow previous *BABAR* analyses [11] and a detailed explanation of particle identification (PID) is given elsewhere [11], [12].

3 ANALYSIS METHOD

This analysis commences with charged and neutral track selections. Each charged track candidate is required to have at least 12 DCH hits and transverse momentum greater than 100 MeV/c. If it is not associated with a K_S^0 decay that track candidate must originate near the nominal beam spot.

A charged-kaon or -pion candidate is selected on the basis of dE/dx information from the SVT and DCH and the Cherenkov angle measured by the DIRC. An electron candidate is required to

have a good match between the expected and measured energy loss $(\mathrm{d}E/\mathrm{d}x)$ in the DCH, and between the expected and measured Cherenkov angle in the DIRC. The ratio of EMC shower energy to DCH momentum, and the number of EMC crystals associated with the track candidate must be appropriate for an electron. A muon is selected on the basis of energy deposited in the EMC, the number and distribution of hits in the IFR, the match between the IFR hits and the extrapolation of the DCH track into the IFR, and the depth of penetration of the track into the IFR.

A photon candidate is identified from energy deposited in contiguous EMC crystals summed together to form a cluster which has total energy greater than 30 MeV and a shower shape consistent with that expected for an electromagnetic shower.

The intermediate states in the neutral $\bar{B}^0/B^0 \to J/\psi\pi^\pm\pi^0 K^\mp$, and charged $B^\pm \to J/\psi\pi^\pm\pi^0 K_S^0$ decay modes used in this analysis are $J/\psi \to e^+e^-$, $J/\psi \to \mu^+\mu^-$, $\pi^0 \to \gamma\gamma$, and $K_S^0 \to \pi^+\pi^-$. They are selected to be within the mass intervals $2.95 < M(e^+e^-) < 3.14$, $3.06 < M(\mu^+\mu^-) < 3.14$, $0.119 < M(\gamma\gamma) < 0.151$, and $0.4917 < M(\pi^+\pi^-) < 0.5037$ GeV/c^2. The e^+e^- mass interval is larger than that for $\mu^+\mu^-$ in order to recover events in which part of the energy was carried away by bremsstrahlung photons. The orientation of the displacement vector between the K_S^0 decay vertex and the J/ψ vertex in the lab is required to be consistent with the K_S^0 momentum direction.

The search for B signal events utilizes two kinematic variables [11]: the energy difference ΔE between the energy of the B candidate and the beam energy E_b^* in the $\Upsilon(4S)$ rest frame; and the beam-energy-substituted mass $m_{\mathrm{ES}} \equiv \sqrt{\left(E_b^*\right)^2 - \left(p_B^*\right)^2}$, where p_B^* is the reconstructed momentum of the B candidate in the $\Upsilon(4S)$ frame. Signal events should have $m_{\mathrm{ES}} \approx m_B$, where m_B is the nominal mass of the B-meson, and $|\Delta E| \approx 0$.

Before the data were analyzed, the selection criteria were optimized and fixed separately for the charged and neutral modes using a Monte Carlo (MC) simulation of signal and known backgrounds. The number of reconstructed MC signal events (n_s^{mc}) and the number of reconstructed MC background events (n_b^{mc}) in the signal-box were used to estimate the sensitivity ratio $n_s^{\mathrm{mc}}/(a/2 + \sqrt{n_b^{\mathrm{mc}}})$ [13], where a, the number of standard deviations of significance desired, was set to 3. Note the maximum of this ratio is independent of the unknown signal branching fraction. This ratio was maximized by varying the selection criteria on ΔE, m_{ES}, the $X(J/\psi\pi^\pm\pi^0)$ mass, the $K_S^0(\pi^+\pi^-)$ mass, the K_S^0 decay length signficance, the $\gamma\gamma$ mass, and the particle identification for electrons, muons and charged kaons. When there are more than one candidate (on average there were 1.3 candidates/event) per event, the candidate with the smallest absolute ΔE value was chosen. All the following plots are displayed with one candidate per event.

The ΔE and m_{ES} data distributions, after applying the optimized cuts for the neutral and charged B modes, are shown in Figs. 1 and 2, respectively. A clear signal peak is observed at zero in the ΔE distribution and near 5.279 GeV/c^2 in the m_{ES} distribution. The other feature in the ΔE plots is a wide peak near 0.2 GeV/c^2 which is due to $B \to J/\psi K^*$ events combined with a random pion track. The rectangular area (signal-box region) bounded by $|m_{\mathrm{ES}} - m_B| < 5$ MeV/c^2 and $|\Delta E| < 20$ MeV was found to be optimal to select signal events. Choosing events in the signal-box region and applying a mass cut of $0.67 < M(\pi^\pm\pi^0) < 0.78$ GeV/c^2 to select the $\rho^\pm$ mass region, the $K^\mp\pi^\pm\pi^0$ mass distributions are shown in Fig. 3 for the charged and neutral B modes. There are clear signal peaks for $K_1^0(1270) \to K^\pm\rho^\mp$ and $K_1^\pm(1270) \to K_S^0\rho^\mp$ corresponding to the decays, $B^\pm \to J/\psi K_1^\pm$ and $B^0 \to J/\psi K_1^0$, previously observed by Belle [14]. In Fig. 3 the dashed histogram background estimates are obtained using the m_{ES} sideband region, $5.24 < m_{\mathrm{ES}} < 5.26$ GeV/c^2. The number of observed K_1 events are consistent with the Belle measurements.

The $J/\psi\pi^\pm\pi^0$ mass spectra from the neutral and charged B modes are shown in Fig. 4. No

charged decay signal, $X^{\pm} \to J/\psi\pi^{\pm}\pi^0$, is evident at 3.872 GeV/c^2. The mass spectra have backgrounds that peak near 3.7 GeV/c^2 and have a step near 4.0 GeV/c^2. From MC studies we find the peak near 3.7 GeV/c^2 is due to $\psi(3686) \to J/\psi\pi\pi$ decays where one pion is exchanged with a random π^0. The step near 4.0 GeV/c^2 is caused by $B \to J/\psi K_1, K_1 \to \rho K$ decays.

4 RESULTS AND SYSTEMATIC UNCERTAINTIES

To extract an upper limit for $X^{\pm} \longrightarrow J/\psi\pi^{\pm}\pi^0$, requires a search for a signal in the $J/\psi\pi^{\pm}\pi^0$ mass, m_{ES}, and ΔE distributions. A signal from $B \longrightarrow X^{\pm}K$, $X^{\pm} \longrightarrow J/\psi\pi^{\pm}\pi^0$ should produce signal peaks in all three distributions. The peaking background from non-resonant, $B \longrightarrow J/\psi\pi^{\pm}\pi^0 K$, would produce peaks in the m_{ES} and ΔE distributions and a flat $J/\psi\pi^{\pm}\pi^0$ mass distribution near 3.872 GeV/c^2. The combinatoric background will not create peaks in any of the three distributions and should produce a m_{ES} distribution whose shape can be parametrized by an ARGUS function [17]. To estimate the number of signal events (n_S), we count the number of observed events (n_{obs}) in the signal region and subtract the estimated number of combinatoric background events (n_{comb}) and the estimated number of peaking background events (n_{peak}).

The number of observed events, n_{obs}, is obtained by counting the number of events satisfying, $|m_{ES} - m_B| < 5$ MeV/c^2, $|\Delta E| < 20$ MeV/c^2, and $\left| \mathrm{M}\left(J/\psi\pi^{\pm}\pi^0 \right) - 3.872 \mathrm{MeV/c}^2 \right| < 12$ MeV/c^2.

The number of combinatoric background events, n_{comb}, is extracted from the m_{ES} distribution obtained after requiring $|\Delta E| < 20$ MeV/c^2, and $\left| \mathrm{M}\left(J/\psi\pi^{\pm}\pi^0 \right) - 3.872 \mathrm{MeV/c}^2 \right| < 12$ MeV/c^2. The $J/\psi\pi^{\pm}\pi^0$ signal band has a 24 MeV/c^2 wide mass window. These m_{ES} distributions for the neutral and charged B modes are separately fit with the sum of a signal Gaussian function and an ARGUS function. The histograms with the fits are shown in Figs. 6 and 7 for the neutral and charged B modes, respectively. The resulting ARGUS function is integrated over the m_{ES} range, $|m_{ES} - m_B| < 5$ MeV/c^2, to produce n_{comb}. The error σ_{comb} is obtained from the fit error on the normalization of the ARGUS function. The resulting values for n_{comb} and σ_{comb} are listed in Table 1.

The number of peaking background events, n_{peak}, is extracted from the m_{ES} distribution obtained after requiring $|\Delta E| < 20$ MeV/c^2, and $48 < \left| \mathrm{M}\left(J/\psi\pi^{\pm}\pi^0 \right) - 3.872 \mathrm{MeV/c}^2 \right| < 72$ MeV/c^2. This $J/\psi\pi^{\pm}\pi^0$ sideband has a 48 MeV/c^2 wide mass window and is twice the mass range of the signal band. These m_{ES} distributions for the neutral and charged B modes are separately fit with the sum of a signal Gaussian function and an ARGUS function. The m_{ES} histograms with the fits are shown in Figs. 6 and 7 for the neutral and charged B modes, respectively. The estimated number of peaking background events , n_{peak}, is calculated by counting the number of events in the $|m_{ES} - m_B| < 5$ MeV/c^2 m_{ES} region, subtracting the number of combinatoric events obtained from integrating the ARGUS function over the same range, $|m_{ES} - m_B| < 5$ MeV/c^2, and finally dividing the result by two. Note the Gaussian has a width that was fixed to a value that determined from a fit to the m_{ES} distribution obtained using both the $J/\psi\pi^{\pm}\pi^0$ signal band and the $J/\psi\pi^{\pm}\pi^0$ sideband. The error σ_{peak} is obtained by adding in quadrature the Poisson errors on the number of events in $|m_{ES} - m_B| < 5$ MeV/c^2 and the fit errors on the normalization of the ARGUS function. The resulting values for n_{peak} and σ_{peak} are listed in Table 1.

The total background (n_b) is the sum of the peaking and combinatoric backgrounds and its error (σ_b) combines in quadrature the errors from the peaking and combinatoric backgrounds. The backgrounds and their errors are summarized in Table 1.

Table 1: Efficiencies, number of signal-box events, and estimated number of background events (peaking, combinatoric, total) for the neutral and charged B decays.

Mode	ϵ	n_{obs}	$n_{peak} \pm \sigma_{peak}$	$n_{comb} \pm \sigma_{comb}$	$n_b \pm \sigma_b$
$J/\psi\pi^\pm\pi^0 K^\mp$	10.65%	87	31.2 ± 8.0	70.6 ± 6.3	101.8 ± 10.2
$J/\psi\pi^\pm\pi^0 K_S^0$	8.50%	31	0.6 ± 4.7	27.0 ± 4.0	27.6 ± 6.2

The efficiencies (ϵ) for the processes, $\bar{B}^0/B^0 \to X^\pm K^\mp$, $X^\pm \to J/\psi\pi^\pm\pi^0$ and $B^\pm \to X^\pm K_S^0$, $X^\pm \to J/\psi\pi^\pm\pi^0$ are determined by MC simulation using an $X^\pm$ signal with zero width, mass 3.872 GeV/c^2 and a model consisting of the sequential isotropic two body decays $B \to X^\pm K$, $X^\pm \to J/\psi\rho^\pm$ and $\rho^\pm \to \pi^\pm\pi^0$. Efficiencies are corrected for the small differences between data and MC by using well-understood control samples where results from data and MC are available. These corrections are applied to PID, neutral detection, and tracking efficiencies. The final efficiencies for each mode are listed in Table 1.

The systematic errors include uncertainties in the number of $B\bar{B}$ events in the data sample, the secondary branching fractions, the MC statistics, the decay model for the generated events, the background parametrization, the particle identification, the charged particle tracking, and the π^0 reconstruction. The individual uncertainties are given as percentages in Table 2. The secondary branching fractions [15] include $\mathcal{B}(J/\psi \to e^+e^-, \mu^+\mu^-)$=0.1181 $\pm$ 0.0014 and $\mathcal{B}(K_S^0 \to \pi^+\pi^-)$=0.686 $\pm$ 0.0027. The decay model uncertainty is estimated by comparing the efficiencies for phase space and different decay models [16] with $J^{PC} = 1^{++}$ and $J^{PC} = 2^{--}$.

Table 2: Percentage Systematic Errors from the neutral and charged B decay modes.

Systematic Errors(%)	$J/\psi\pi^\pm\pi^0 K^\mp$	$J/\psi\pi^\pm\pi^0 K_S^0$
No. of $B\bar{B}$ events	1.1	1.1
Branching fractions	5.3	5.3
MC statistics	2.1	2.3
MC decay model	1.1	3.0
Bkgd sideband width	0.8	1.9
Particle ID	5.0	5.0
Tracking $\pi^\pm$	1.4	1.4
Tracking $K^\pm$	1.4	-
Tracking K_S^0	-	2.6
Tracking $J/\psi \to e^+e^-, \mu^+\mu^-$	1.8	1.8
π^0 correction	3.2	3.2
TOTAL (σ_{sys})	8.8	9.7

The background parametrization uncertainty is estimated by varying the background sideband width, refitting the $m_{\rm ES}$ distributions, and recalculating the number of events. The uncertainties in particle identification, charged tracking efficiency and π^0 reconstruction efficiency are determined by studying control samples [11]. The total fractional errors (σ_{sys}) listed at the bottom of Table 2, are determined by adding the individual contributions in quadrature.

The probability distribution of the signal events is modeled as a Gaussian with a mean (n_s) and sigma (σ_s). For each B-decay mode the mean is $n_s = n_{obs}$ - n_b and the sigma is $\sigma_s = \sqrt{n_{obs} + \sigma_b^2}$

11

$\times \sqrt{1 + \sigma_{sys}^2}$. The systematic error is added in quadrature and scales the errors on n_{obs} and n_b by the same fraction. The results are listed in Table 3. We note the mean values, n_s, for the charged and neutral modes are consistent within errors to zero signal events.

The 90% confidence level (C.L.) upper limit number of events (N_{90}) is calculated using the Gaussian probability distribution with the assumption the number of signal events is always greater than zero. The integral of the distribution from zero to N_{90} will be 90% of the total area above zero. Combining N_{90}, ϵ, $N_{B\bar{B}}$ events, and the secondary branching fractions, we obtain,

$$\mathcal{B}(\bar{B}^0/B^0 \to X^\pm K^\mp, X^\pm \to J/\psi\pi^\pm\pi^0) \quad < \quad \frac{N_{90}}{\epsilon N_{B\bar{B}}\mathcal{B}(J/\psi \to l^+l^-)}$$

$$= \quad 5.8 \times 10^{-6} \quad (90\% \ C.L.),$$

$$\mathcal{B}(B^\pm \to X^\pm K_S^0, X^\pm \to J/\psi\pi^\pm\pi^0) \quad < \quad \frac{N_{90}}{\epsilon N_{B\bar{B}}\mathcal{B}(J/\psi \to l^+l^-)\mathcal{B}(K_S^0 \to \pi^+\pi^-)}$$

$$= \quad 11 \times 10^{-6} \quad (90\% \ C.L.).$$

for the neutral and charged branching fraction upper limits. For completeness we include the central value (68% confidence interval) for the branching fraction using the $n_s \pm \sigma_s$ values,

$$\mathcal{B}(\bar{B}^0/B^0 \to X^\pm K^\mp, X^\pm \to J/\psi\pi^\pm\pi^0) \quad = \quad \frac{n_s \pm \sigma_s}{\epsilon N_{B\bar{B}}\mathcal{B}(J/\psi \to l^+l^-)}$$

$$= \quad (-5.5 \pm 5.2) \times 10^{-6},$$

$$\mathcal{B}(B^\pm \to X^\pm K_S^0, X^\pm \to J/\psi\pi^\pm\pi^0) \quad = \quad \frac{n_s \pm \sigma_s}{\epsilon N_{B\bar{B}}\mathcal{B}(J/\psi \to l^+l^-)\mathcal{B}(K_S^0 \to \pi^+\pi^-)}$$

$$= \quad (2.3 \pm 5.7) \times 10^{-6}.$$

The results are summarized in Table 3.

Table 3: The estimated number of signal events, 90% C.L. upper limit of signal events, the branching fraction upper limits, and the branching fraction ($\mathcal{B}$) for each B-decay.

Mode	$n_s \pm \sigma_s$	N_{90}	90% C.L.	$\mathcal{B}$
$J/\psi\pi^\pm\pi^0 K^\mp$	-14.8 ± 13.9	15.6	$< 5.8 \times 10^{-6}$	$(-5.5 \pm 5.2) \times 10^{-6}$
$J/\psi\pi^\pm\pi^0 K_S^0$	3.4 ± 8.3	15.9	$< 11 \times 10^{-6}$	$(2.3 \pm 5.7) \times 10^{-6}$

5   PHYSICS INTERPRETATION

We test the charged partner hypothesis at a mass of 3872 MeV/c^2 using a likelihood ratio test [15]. Here we determine the ratio of the two probabilities from the null (H_0) and signal (H_1) hypotheses using our experimental observation of 87 events in the signal-box.

The null hypothesis assumes the estimated background events, $n_b \pm \sigma_b$, produced all the observed signal-box events. Assuming the background probability distribution is a Gaussian function, we calculate a probability of $P(H_0)=7.34 \times 10^{-2}$ to measure 87 or fewer events.

The isovector signal hypothesis predicts the product branching fractions to have the ratio, $\mathcal{B}(B \to X^\pm K, X^\pm \to J/\psi\rho^\pm) =2 \ \mathcal{B}(B \to X(3872)K, X(3872) \to J/\psi\rho^0)$. Using the *BABAR* branching fractions $\mathcal{B}(B^\pm \to X(3872)K^\pm, X(3872) \to J/\psi\pi^+\pi^-) = (1.28 \pm .41) \times 10^{-5}$ and assuming all the $\pi^+\pi^-$ decays originate from ρ^0, we expect $\mathcal{B}(B \to X^\pm K^\mp, X^\pm \to J/\psi\rho^\pm) = (2.56 \pm 0.82) \times 10^{-5}$. This would produce 69 ± 23 observed signal events in a data sample of 213 million $B\bar{B}$ events. The error combines the uncertainty on the branching fraction and the systematic error, σ_{sys}, on our efficiency. The probability distributions for the signal events and the

estimated background events are modeled as two uncorrelated Gaussian functions. The probability of observing 87 or fewer events with this probability distribution is $P(H_1){=}1.18 \times 10^{-4}$.

The likelihood ratio (λ) test of the null hypothesis relative to the signal hypothesis yields $\lambda = P(H_0)/P(H_1) = 622$. This corresponds to a probability of less than 1 part in 600 that the $X^{\pm}$ hypothesis is correct with the outcome of our measurement. Hence our result does not support the existence of charged molecular states or charged partners of the $X(3872)$.

6 SUMMARY

In conclusion, we have performed a search for a charged partner of the $X(3872)$ decaying to $J/\psi \pi^{\pm}\pi^0$. Our results set upper limits on the product branching fractions of $\mathcal{B}(\bar{B}^0/B^0 \to X^{\pm}K^{\mp}, X^{\pm} \to J/\psi\pi^{\pm}\pi^0) < 5.2 \times 10^{-6}$ and $\mathcal{B}(B^{\pm} \to X^{\pm}K^0_S, X^{\pm} \to J/\psi\pi^{\pm}\pi^0) < 11 \times 10^{-6}$ at the 90% confidence level. We exclude the isovector X hypothesis with a likelihood ratio test and with our experimental results we obtain a ratio greater than 600 for the null hypothesis relative to the isovector signal hypothesis.

7 ACKNOWLEDGMENTS

References

[1] Belle Collaboration, S.K. Choi *et al.*, Phys. Rev. Lett. **91**, 262001 (2003).

[2] CDF Collaboration, submitted to Phys. Rev. Lett., December 5, 2003, hep-ex/0312021.

[3] D0 Collaboration, submitted to Phys. Rev. Lett., May 4, 2004, hep-ex/0405004.

[4] BaBar Collaboration, submitted to Phys. Rev. Lett., June 7, 2004, hep-ex/0406022.

[5] C. Quigg, April 22, 2004, hep-ph/0403187; E. Swanson, June 7, 2004, hep-ph/0406080; C. Quigg, July 10, 2004, hep-ph/0407124.

[6] E. Eichten, K. Lane, and C. Quigg, Phys. Rev. Lett. **89**, 162002 (2002); T. Barnes and S. Godfrey, Phys.Rev.D **69**, 054008 (2004).

[7] N. Tornqvist, Phys. Lett. B **590**, 209 (2004); M. B. Voloshin, Phys. Lett. B **579**, 316 (2004); F. Close and P. Page, Phys. Lett. B **578**, 119 (2004); C.Y. Wong, Phys. Rev. C **69**, 055202 (2004); E. Braaten and M. Kusunoki, Phys. Rev. D **69**, 074004 (2004); E. Swanson, Phys. Lett. B **588**, 189 (2004).

[8] F. Close and S. Godfrey, Phys. Lett. B **574**, 210 (2003).

[9] E. Eichten, K. Lane, and C. Quigg, Phys. Rev. D **69**, 094019 (2004).

[10] *BABAR* Collaboration, B. Aubert *et al.*, Nucl. Instr. and Methods A **479**, 1 (2002).

[11] *BABAR* Collaboration, B. Aubert *et al.*, Phys. Rev. D **65**, 032001 (2002). This publication forms a basic reference of our analysis. The particle identification and tracking criteria for the photons, electrons and muons are given in sections IIC and IID. The photon candidates selection is described in section VC. The electron candidates are required to satisfy the "Tight" and "Loose" selections and the muon candidates use the "Loose" selections, as specified in Table II. The estimate of the efficiency uncertainty in the PID, tracking and photon detection using control samples from data is described in section XI.

[12] *BABAR* Collaboration, B. Aubert *et al.*, Phys. Rev. D **66**, 032003, (2002). The charged kaon candidate used a selection slightly more stringent than that described in this reference.

[13] G. Punzi, "Sensitivity of searches for new signals and its optimization," eprint physics/0308063, August 2003.

[14] Belle Collaboration, K. Abe *et al.*, Phys. Rev. Lett. **87**, 161601 (2001).

[15] Particle Data Group, K. Hagiwara *et al.*, Phys. Rev. D **66**, 010001 (2002), see section 31.3.1 for a discussion of the likelihood ratio test.

[16] S. Pakvasa and M. Suzuki, Phys. Lett. B **579**, 67 (2004). Note that the authors assume the relative orbital angular momentum between the J/ψ and the di-pion state is $L = 0$. This is justified for di-pion events near the kinematic limit.

[17] The original ARGUS function is described in H. Albrecht *et al.*, Phys. Lett. B **185**, 218 (1987) and Phys. Lett. B **241**, 278 (1990).
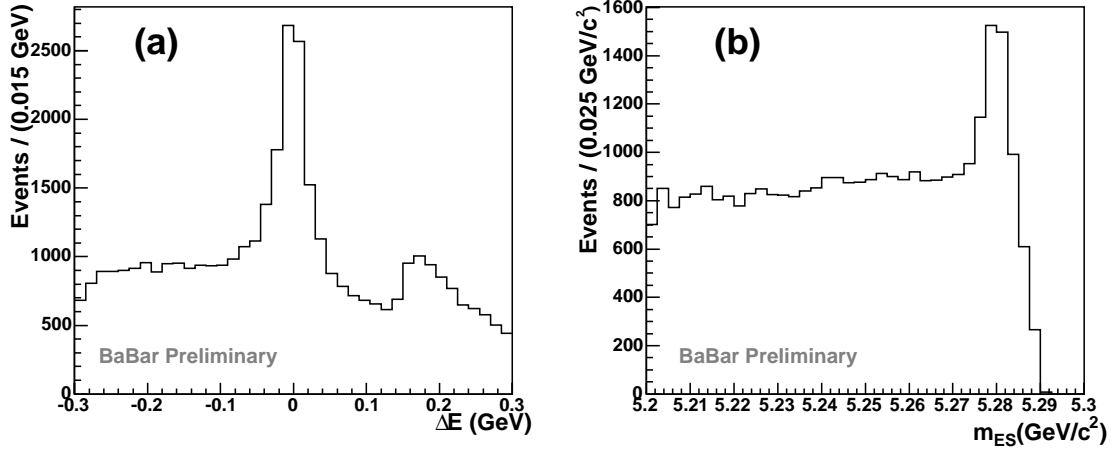
FIGURES

Figure 1: The ΔE (a) and m_{ES} (b) distributions from the $\bar{B}^0/B^0 \to J/\psi\pi^\pm\pi^0 K^\mp$ mode after applying the optimized cuts.
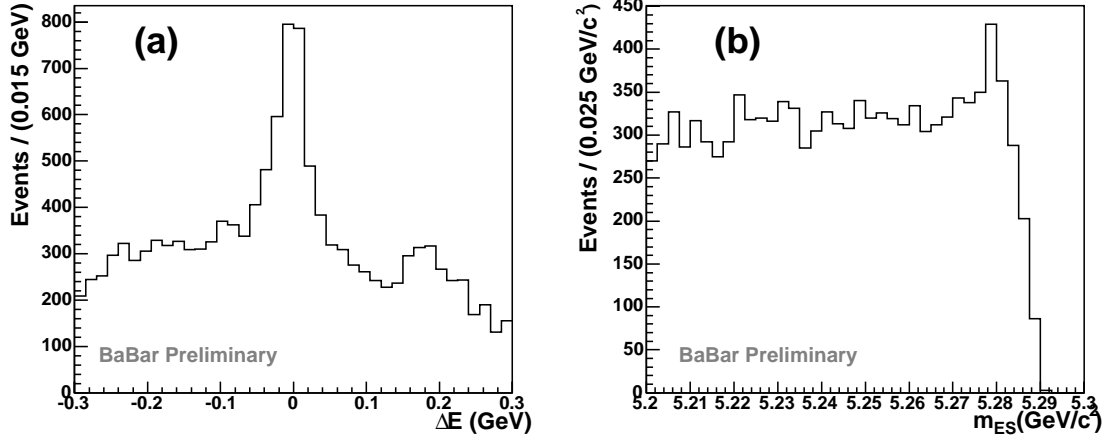

Figure 2: The ΔE (a) and m_{ES} (b) distributions from the $B^\pm \to J/\psi\pi^\pm\pi^0 K_S^0$ mode after applying the optimized cuts.
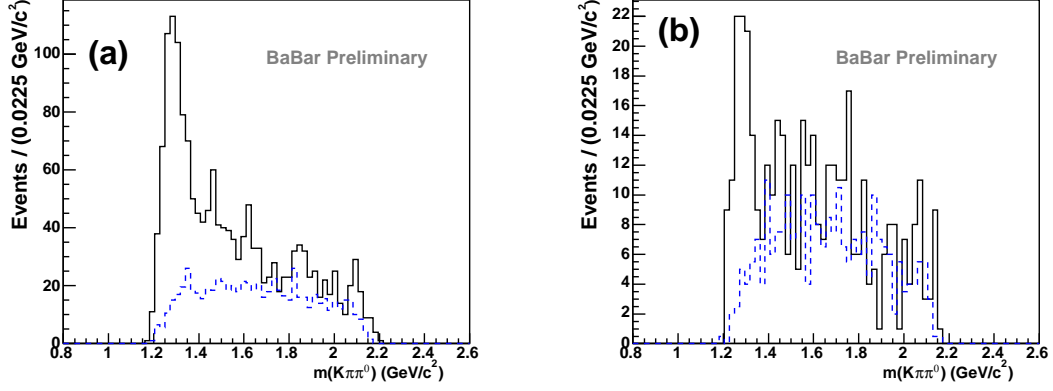
Figure 3: The $\pi^{\pm}\pi^0 K^{\mp}$ (a) distributions from the $\bar{B}^0/B^0 \to J/\psi\pi^{\pm}\pi^0 K^{\mp}$ mode and the $\pi^{\pm}\pi^0 K^0_S$ (b) distributions from the $B^{\pm} \to J/\psi\pi^{\pm}\pi^0 K^0_S$ mode after a signal-box and a $\rho^{\pm}$ mass cut. The dashed histogram is obtained from events in a $5.24 < m_{ES} < 5.26$ GeV/c^2 sideband. The neutral and charged $K_1(1270)$ signals are evident in the plots (a) and (b), respectively.
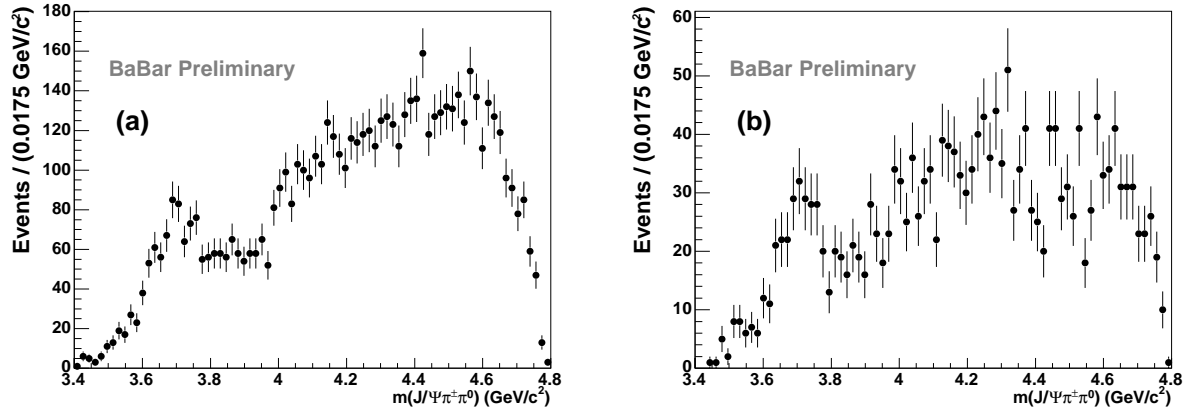

Figure 4: The $J/\psi\,\pi^{\pm}\pi^0$ invariant mass from neutral (a), $\bar{B}^0/B^0 \to J/\psi\pi^{\pm}\pi^0 K^{\mp}$, and charged (b), $B^{\pm} \to J/\psi\pi^{\pm}\pi^0 K^0_S$, modes.
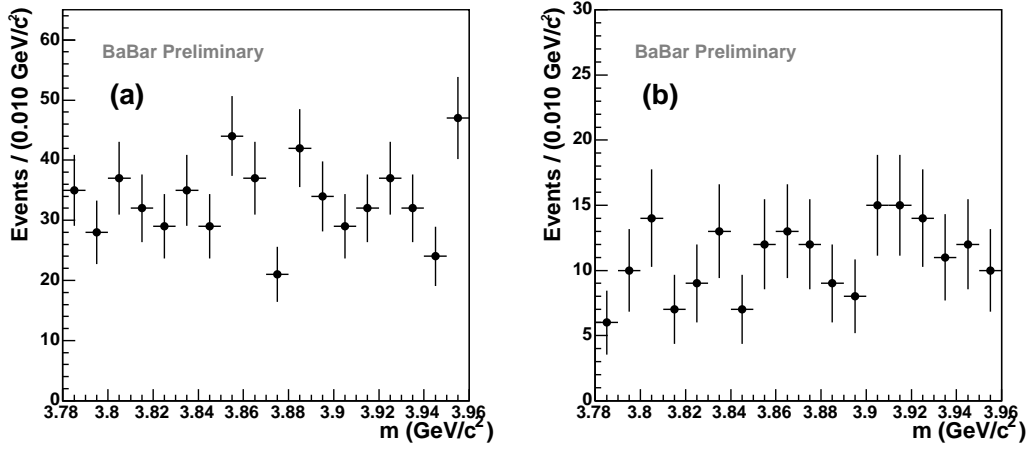
Figure 5: The $J/\psi\pi^\pm\pi^0$ invariant mass in 10 MeV/c^2 bins for the neutral (a), $\bar{B}^0/B^0 \to J/\psi\pi^\pm\pi^0 K^\mp$, and charged (b), $B^\pm \to J/\psi\pi^\pm\pi^0 K^0_S$, modes. These plots are the same as the previous Figs. except they have finer binning. No evidence for the charged $X(3872)$ partner is observed in either plot.
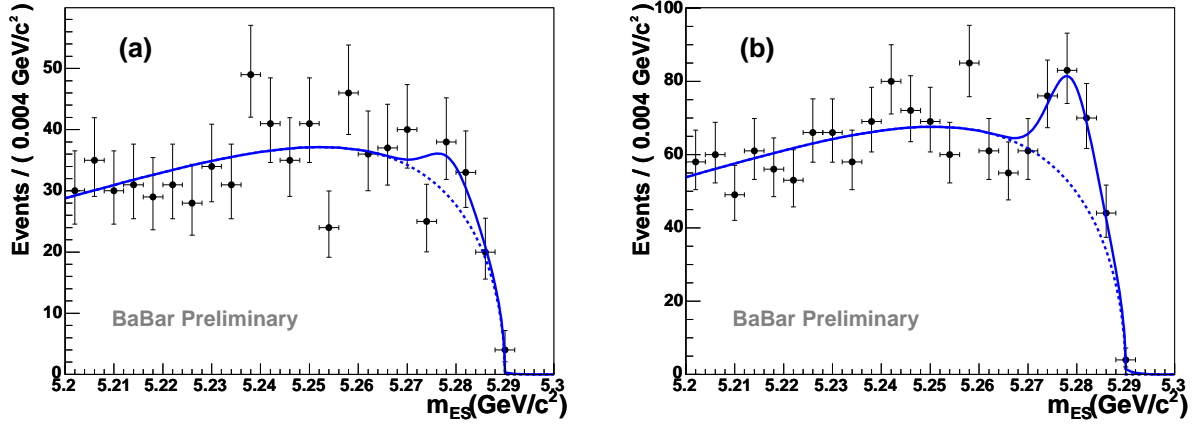

Figure 6: Fitted m_{ES} distribution for the B^0 mode with the $X^\pm$ signal region selection, $|m(J/\psi\pi^\pm\pi^0) - 3872\,\mathrm{MeV}/c^2| < 12\,\mathrm{MeV}/c^2$, (a) and with the sideband region selection, $48 < |m(J/\psi\pi^\pm\pi^0) - 3872\,\mathrm{MeV}/c^2| < 72\,\mathrm{MeV}/c^2$, (b). The signal region selection plot is used to estimate the combinatoric background. The sideband region selection plot is used to estimate the peaking background. The sideband region selection has twice the $J/\psi\pi^\pm\pi^0$ mass range of the signal region selection.
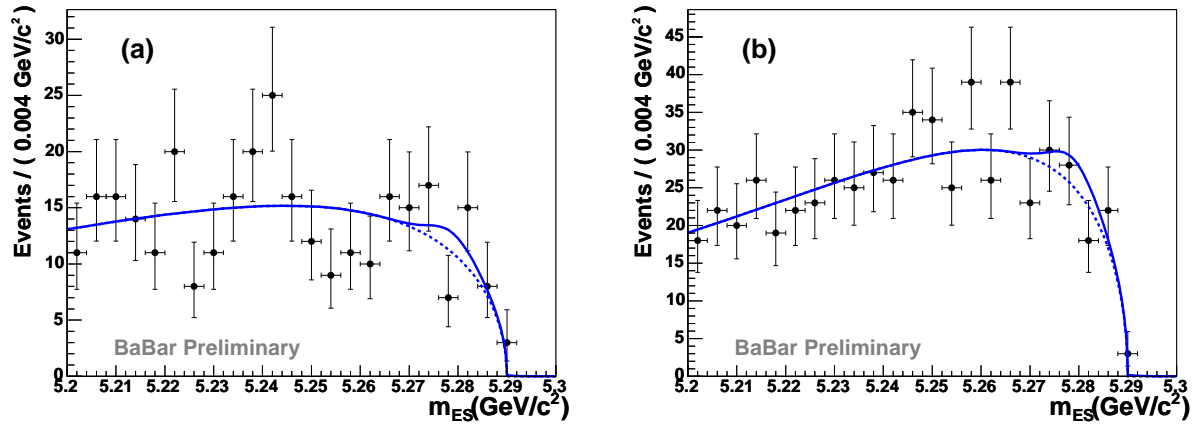
Figure 7: Fitted m_{ES} distribution for the $B^{\pm}$ mode with the $X^{\pm}$ signal selection, $|m(J/\psi\,\pi^{\pm}\pi^{0}) - 3872\,\mathrm{MeV}/c^2| < 12\,\mathrm{MeV}/c^2$, (a) and with the sideband region selection, $48 < |m(J/\psi\,\pi^{\pm}\pi^{0}) - 3872\,\mathrm{MeV}/c^2| < 72\,\mathrm{MeV}/c^2$, (b). The signal region selection plot is used to estimate the combinatoric background. The sideband region selection plot is used to estimate the peaking background. The sideband region selection has twice the $J/\psi\pi^{\pm}\pi^{0}$ mass range of the signal region selection.